NASA TECHNICAL NOTE

NASA TN D-3336

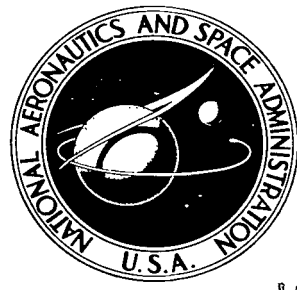

NASA TN D-3336

BENDING TESTS OF LARGE-DIAMETER RING-STIFFENED CORRUGATED CYLINDERS

by James P. Peterson and James Kent Anderson

Langley Research Center
Langley Station, Hampton, Va.

NATIONAL AERONAUTICS AND SPACE ADMINISTRATION • WASHINGTON, D. C. • MARCH 1966

NASA TN D-3336

BENDING TESTS OF LARGE-DIAMETER RING-STIFFENED CORRUGATED CYLINDERS

By James P. Peterson and James Kent Anderson

Langley Research Center
Langley Station, Hampton, Va.

NATIONAL AERONAUTICS AND SPACE ADMINISTRATION

For sale by the Clearinghouse for Federal Scientific and Technical Information
Springfield, Virginia 22151 – Price $0.45

BENDING TESTS OF LARGE-DIAMETER RING-STIFFENED CORRUGATED CYLINDERS

By James P. Peterson and James Kent Anderson
Langley Research Center

SUMMARY

Results of bending tests on five ring-stiffened corrugated cylinders are presented. The cylinders failed by buckling into a general-instability mode involving buckling of the corrugated wall and reinforcing rings as a composite wall. Buckling in this mode occurred at a load approximately 75 percent of the load computed with the use of a small-deflection buckling theory for cylinders in bending. One of the test cylinders buckled into a panel-instability mode (buckling of corrugated wall between stiffening rings) prior to buckling into the general-instability mode. Buckling in the panel-instability mode was accurately predicted with the use of the theory.

INTRODUCTION

Contemporary launch-vehicle designs make use of the ring-stiffened corrugated cylinder as an intertank or interstage structure (ref. 1). The principal structural function of the corrugated cylinder, when used in this capacity, is to transmit thrust loads to the upper structure and to withstand aerodynamic loads, particularly those which result in bending loads. The capacity of stiffened cylinders to withstand loads which cause compressive stresses in the wall of the cylinders is normally computed by design equations which neglect the effect of eccentricity (one-sidedness) of the stiffening elements on buckling strength. References 2 to 4 point out that such neglect leads to large errors in the predicted strength of corrugated cylinders and present design equations which take into account eccentricity effects. In addition, reference 2 presents data on compression tests of corrugated cylinders which agree well with theoretical predictions.

The purpose of the present paper is to report the results obtained from bending tests of five corrugated cylinders stiffened with small, closed, hat-section rings. The only structural variable in the test cylinders was ring spacing which was varied over a sufficiently wide range to include modes of buckling that entailed both buckling of the wall between rings (panel instability) and buckling of the wall and rings as a composite wall (general instability). Results from the tests are discussed with the aid of the buckling analyses of references 2 to 4.

SYMBOLS

The units used for physical quantities defined in this paper are given both in the U.S. Customary Units and in the International System of Units (SI) (ref. 5). Factors relating the two systems are given in appendix A.

b — width of flat plate element of idealized corrugation in which radii of curvature between flat elements are zero, $\frac{p}{2(1 + \cos \phi)}$

D_x, D_y — bending stiffness of corrugated cylinder wall in axial and circumferential direction, respectively

D_{xy} — twisting stiffness of corrugated cylinder wall

E — Young's modulus

E_x, E_y — extensional stiffness of corrugated cylinder wall in axial and circumferential direction, respectively

G — shear modulus

G_{xy} — in-plane shear stiffness of corrugated cylinder wall

I_{ring} — moment of inertia of reinforcing ring about axis perpendicular to generator of cylinder

l — ring spacing (see fig. 2)

M — bending moment applied to test cylinder

m — number of half-waves in cylinder buckle pattern in axial direction of cylinder

N_x — load per unit length of cylinder circumference at buckling

$N_O = \frac{\pi^2 D_x}{l^2}$

n — number of full waves in cylinder buckle pattern in circumferential direction of cylinder loaded in compression

p	pitch of corrugation (see fig. 2)
R	radius of cylinder measured to centroid of corrugated wall
t	sheet thickness of material of corrugated wall of cylinder (see fig. 2)
$u = \frac{\pi}{2}\sqrt{\frac{N_x}{N_o}}$	
θ	angle of rotation
μ	Poisson's ratio of corrugation material
μ_x, μ_y	Poisson's ratio associated with bending of corrugated wall of cylinder in axial and circumferential direction, respectively
μ_x', μ_y'	Poisson's ratio associated with extension of corrugated wall of cylinder in axial and circumferential direction, respectively
ϕ	corrugation angle (see fig. 2)

Subscripts:

cr	critical
cyl	cylinder
ring	reinforcing ring
ult	ultimate

TEST SPECIMENS AND TEST PROCEDURE

General features of the test cylinders are depicted in figure 1 and details of the cylinders are given in figure 2 and table I. The cylinders were constructed from 7075-T6 aluminum-alloy sheet material. Each cylinder had seven longitudinal wall splices that consisted of lap joints held together by double rows of spot welds, and had three circumferential splices in each stiffening ring that were stiffened locally with the use of a double thickness of material. The wall splices and ring splices were placed so that neither was near the section of the cylinder subjected to highest compressive stresses.

A survey of the skin thickness of each cylinder was obtained by micrometer measurement; the values of skin thickness given in table I correspond to an average value of many measurements. The corrugation geometry and ring geometry were checked only for certain cylinders. The other cylinders were fabricated with the use of the same dies and were presumed to be fabricated to the same accuracy. The checks that were made indicated that actual dimensions were in close agreement with the nominal values given in figure 2. For instance, measurements of corrugation geometry were made from a trace of the corrugated wall obtained by cutting a section of the corrugated wall from a test cylinder and by tracing its outline on paper. Measurements of the outline indicated that the wave length of the corrugations was within 2 percent of the nominal value and that the depth of corrugations and the corrugation angle ϕ were equal to the nominal value within the accuracy of such measurements.

The test section of the cylinders was 80 inches (2.03 m) long and was terminated at each end by heavy hat-section rings (figs. 1(b) and 2). Outside the test section, double-thickness walls were used to prevent failures from occurring in these areas. The double thickness was obtained by nesting an extra corrugated sheet with the corrugated wall and by bonding and riveting the wall and sheet together in the nested position.

The various test cylinders were obtained by constructing cylinders with different numbers of equally spaced stiffening rings in the test section. Cylinders were built with 3, 5, 7, 9, and 19 stiffening rings.

Typical material properties were used in reducing data from the tests. Young's modulus E was taken to be 10 500 ksi (72.4 GN/m^2) and Poisson's ratio μ was assumed to be 0.32.

The test cylinders were loaded in bending through a loading frame with the use of a hydraulic testing machine. The test setup is shown in figure 3. The presence of stray loads in the test cylinders was minimized insofar as practicable by employing rollers between moving surfaces and by counterbalancing fixtures near their center of gravity. Rollers were used between the loading frame and the floor supports as well as between the loading frame and the testing machine. Use of the rollers allows the cylinders to shorten during application of load and helps to restrict the loads at the roller locations to normal loads. The rollers were case hardened, as were the surfaces against which they reacted.

Resistance-type wire strain gages were mounted in a "back-to-back" position at various locations on the test cylinders prior to testing, and strains from the gages were recorded during each test with the use of the Langley central digital data recording facility. Data from the gages were used to determine the strain distribution in the cylinders under load and to help detect buckling of the cylinders.

TEST RESULTS AND DISCUSSION

The moments at which the test cylinders buckled and failed (reached ultimate moment) are given in table I. The values given for buckling were determined from strain-gage measurements taken during the test. Buckles normally developed gradually without abrupt changes in applied load (moment) in the early stages of buckling, and buckling was assumed to have occurred when the strain gages on the cylinder wall in the vicinity of the buckles experienced bending strains from buckle growth of sufficient magnitude to reverse the rate of strain on one side of the wall. The corresponding load is sometimes called the "strain reversal" load (ref. 6). Buckling loads as determined by strain reversal were usually only a few percent less than the failing loads of the cylinders. A notable exception is the buckling load of cylinder 1 which buckled by panel instability at a load approximately 75 percent of the load at which failure finally occurred. Panel instability in this cylinder was followed by general instability buckling that resulted from a redistribution and reshaping of buckles with an increase in applied load; the new buckled configuration entailed buckle-like deformations of the corrugated wall and stiffening rings as a composite wall. (See fig. 4(a) which shows cylinder 1 in an advanced stage of the general-instability mode.) The cylinder failed at a load not much greater than the general-instability load.

Typical failures in other test cylinders are shown in figures 4(b) and 4(c). In each instance, failure resulted from a growth of buckles with load. Growth was accompanied in some instances by a shifting and/or change in buckle shape. Failure was generally not catastrophic even though it entailed a rapid growth of buckles and an accompanying loss in resistance to the applied load. The test cylinders generally appeared undamaged when viewed from the outside after load on the cylinders had been removed and the buckles in the cylinder had disappeared; however, the reinforcing rings generally had sharp crimps at locations of outward buckles. An exception to this behavior was exhibited by cylinder 5, the cylinder with the highest stress level at failure. Failure in cylinder 5 occurred more abruptly than in the other cylinders and was accompanied by a loud resounding noise and by a sharp falling off in applied load with some tearing and crimping of the corrugated skin (fig. 4(c)).

Pertinent results from table I are given in figure 5 for comparison with buckling loads calculated with the use of various theories and with the following orthotropic constants:

$$\left.\begin{aligned} E_x &= \frac{2Et}{1 + \cos \phi} \\ E_y &= \frac{Et^3}{4b^2(1 - \cos \phi)} \end{aligned}\right\} \qquad (1)$$

(Equations continued on next page)

$$
\left.
\begin{aligned}
G_{xy} &= \frac{Gt(1 + \cos \phi)}{2} \\
D_x &= \frac{Etb^2}{3}(1 - \cos \phi) \\
D_y &= \frac{Et^3}{12}\left(\frac{1 + \cos \phi}{2}\right) \\
D_{xy} &= \frac{Gt^3}{12}\left(1 + \frac{2}{1 + \cos \phi}\right) \\
\mu_x' &= \mu \\
\mu_y' &= \mu_x' \frac{E_y}{E_x} \\
\mu_x &= \mu_y = 0
\end{aligned}
\right\} \qquad (1)
$$

The equations for the constants E_y and D_y result from a consideration of the bending deformation of the corrugated plate when loaded by a stretching or bending load in a direction perpendicular to the corrugations. The expression for the constant D_{xy} is a result of the application of equation (b) of reference 7, page 471, to the corrugated plate. The values for Poisson's ratios associated with extension, μ_x' and μ_y', follow from the supposition that an unrestrained plate loaded to a given strain in the direction of its corrugations will experience the same transverse deformation that a noncorrugated plate would experience. Poisson's ratios associated with bending were taken to be zero for lack of a better value. The equations for the remaining constants are commonly used for these quantities (see ref. 3, for example).

The solid-line curves of figure 5 were computed with the use of reference 4 and apply to cylinders like the test cylinders which are loaded in bending. The dash-line curves apply to cylinders loaded in compression; they are included in figure 5 because cylinders in bending are often analyzed for buckling with the use of compression theories. The difference between the bending curve and the compression curve for general-instability buckling is rather large (fig. 5). This difference was noted in references 2 and 4 for other corrugated cylinders and contrasts with the results of earlier studies in which little difference was found between the theoretical buckling loads of cylinders in bending and cylinders in compression for conventional thin-wall cylinders (refs. 8 and 9) and for isotropic sandwich cylinders (ref. 10).

The test cylinders that buckled in the general-instability mode buckled at loads somewhat less (≈10 percent less) than the theoretical buckling load for cylinders loaded by uniform compression and considerably less (≈25 percent less) than the theoretical

buckling load for cylinders loaded in bending. In contrast, reference 2 reports the results of calculations of the buckling load of corrugated cylinders in bending and compression in which good agreement was obtained with results of tests. One reason for the difference between the present results and those of reference 2 may be the values for geometric stiffnesses employed in the calculations. In the present calculations, equations (1) were used to calculate the wall stiffnesses, and the rings were treated as closed tubes in calculating the ring torsional stiffness. In addition, measured values of skin thickness were used in the calculations, and test loads somewhat less than the failing loads were used as the buckling loads. Calculations are often made with the use of more approximate and more conservative values for some of the geometric properties and the resulting calculations compared with the failing load. Differences in such details are believed to account for the discrepancy between the agreement obtained herein and that obtained in reference 2. The two methods of calculation were shown to be equivalent in reference 3 for a different loading and a different type of structure except for differences in details of defining stiffnesses.

The rather sizable discrepancy between theory and experiment shown in figure 5 for general-instability buckling indicates that the buckling behavior of the cylinders is not adequately predicted by the theory of reference 4 and that further work is needed before the behavior of the cylinders is fully understood. It is not clear at this time whether the discrepancy results from some peculiar behavior of corrugated cylinders or whether similar discrepancies might be expected for more conventionally stiffened cylinders. The answer to this question must await further tests and/or a comprehensive re-analysis of existing test data with the use of the newer theories.

Two supplementary tests were conducted on certain test cylinders to help isolate the reason for the 25-percent discrepancy between theory and experiment noted in figure 5. In the first test, a small torsional load was applied to one of the test cylinders prior to loading the cylinder in bending in order to determine the shear stiffness of the corrugated wall. The shear stiffness of corrugated sheet is strongly dependent upon conditions at the ends of the corrugations and can deviate considerably from the elementary calculated value if the ends of the corrugations are not restrained against rolling. (See ref. 11 for a discussion of this behavior in connection with the determination of the twisting stiffness for corrugation-stiffened flat plates.) Twist of the cylinder was measured with Tuckerman optical strain gages and compared with the twist expected on the basis of a calculation using the classic Bredt torsion equation and the elementary value for shear stiffness of the wall (eqs. (1)). The test indicated that the measured stiffness was 88 percent of the elementary calculated stiffness. The elementary stiffness was used in all buckling calculations shown, but check calculations indicated that the predicted loads would be only 2 percent lower if the measured stiffness were used.

The second test consisted of making an appraisal of the effect of the attachment between the stiffening rings and the corrugated cylinder on the buckling load of the cylinder. For this purpose one of the cylinders was retested after attachment clips had been added between the rings and the corrugated wall (fig. 6) to stiffen the attachment. (The test was prompted by ref. 2 which emphasizes the importance of a good attachment and includes a means of incorporating the effect of a weak attachment in a buckling analysis.) The cylinder was rotated 180° from its position in the test fixture in the original test (fig. 3) so that the side that was in tension in the original test was in compression in the auxiliary test. The cylinder failed at essentially the same load in the auxiliary test as it did in the original test, which indicates that the clips were rather ineffectual in changing the buckling load. The design of the clips was such that they were expected to increase the bending and axial stiffness of the ring somewhat and to restrict considerably possible deformations between the outer corrugation crests and the reinforcing rings. Evidently restriction of such deformations is not an important consideration in cylinders of the proportions tested.

Other factors which may influence the agreement between theory and test are shortcomings of the theory in accounting for such things as discrete rings, boundary conditions at the ends of the cylinder, initial imperfections, and prebuckling deformations. Each of these factors is discussed briefly. Discussion of discrete rings and boundary conditions follows immediately and a discussion of initial imperfections and prebuckling deformations is given with the presentation of load-strain plots for the test cylinders.

The effect of not considering the discreteness of reinforcing rings in the calculations for buckling load can be associated with three phenomena: (1) that associated with errors in the "distributed ring-stiffness" approach, such as used herein, when the number of axial half-waves in the buckle pattern is not very different from the number of reinforcing rings in the cylinder, (2) that associated with the method of distributing the ring stiffness in calculations for cylinders with few stiffening rings, and (3) that associated with the prebuckling deformations in the neighborhood of the discrete rings. An indication of the importance of the first two phenomena can be obtained from the study of stiffened cylinders of reference 12, but the importance of the third phenomenon has been studied only for conventional thin-wall cylinders. Discussion of this item is deferred to the general discussion of prebuckling deformations.

The calculations of reference 12 indicate that insignificant errors in calculated buckling load resulted from the use of a distributed stiffness analysis in lieu of a discrete-ring analysis for (1) cylinders buckling into one less half-wave than the number of stiffening rings and (2) cylinders with as few stiffening rings as two. Because both conditions are more severe than those posed by the test cylinders, significant errors from this source are not expected. The contribution of the stiffening rings in the calculated

results presented in figure 5 was obtained by dividing pertinent ring stiffnesses by ring spacing. An alternate and more conservative procedure would be to multiply the ring stiffnesses by the number of rings and divide the resulting product by the length of the test section. Considerably different results would be obtained from the two procedures for cylinders with a small number of stiffening rings. The procedure used was chosen on the basis of the investigation of reference 12 which demonstrated that the procedure gave results in good agreement with a discrete-ring analysis, whereas the alternate procedure did not.

Errors in the predicted buckling loads of figure 5 resulting from the use of boundary conditions not representative of those of the test cylinders may be significant. Recent studies on conventional thin-wall cylinders (refs. 13 to 15) have demonstrated that the choice of boundary conditions in buckling analyses can influence considerably the magnitude of the calculated buckling load. Whether vanishing or nonvanishing circumferential displacements at the ends of the cylinder were used was found to be particularly important; the choice of displacements was more important with boundary conditions characteristic of simply supported cylinders than with boundary conditions characteristic of clamped cylinders (ref. 15).

Detail design at the ends of the test cylinders (fig. 2) was not fashioned to justify the assumption of either clamped or simply supported ends. Instead the test cylinders were made long in an attempt to avoid large errors from this source. In this respect calculations indicate that the cylinders buckled into three or more half-waves in the axial direction, a sufficient number so that significant differences would not normally be expected between calculations employing clamped and simply supported boundary conditions. On the other hand, if the prevention of circumferential displacements is important in corrugated cylinders as it evidently is in conventional cylinders, significant errors in calculated buckling loads for the test cylinders may result from this source. Circumferential displacements of the "middle surface" of the corrugated wall were not prevented in the test cylinders.

Load was introduced into the test cylinders through a steel attachment ring which had a diameter somewhat less than the mean diameter of the corrugated cylinders (see fig. 2); hence, load was introduced eccentrically which tended to bend the compression portion of the cylinder wall outward near the station of attachment. However, design of the cylinder wall near the attachment was such that the bending probably did not carry over into the test section of the cylinder. Some support for this premise was obtained from the strain-gage data obtained during the cylinder tests; the data showed no evidence of bending from load eccentricity, and load eccentricity is not believed to be a significant factor in the discrepancy between theory and test noted in figure 5.

Reasonably good agreement between theory and experiment (fig. 5) was obtained for the cylinder which buckled originally in the panel-instability mode (cylinder 1). Theory for this mode reduces, for all practical purposes, to a calculation wherein the cylinder is considered simply supported at each ring and behaves as a flat corrugated plate (column) between rings (ends); that is, the small circumferential stiffness of the corrugated wall is insufficient to bring into play cylinder effects and the curved wall behaves in much the same manner as the corresponding flat corrugated plate. This behavior allows a rather simple yet rather precise check to be made on the accurateness of the simple-support assumption. The equations necessary for making this check are given in appendix B. A calculation using the equations of appendix B indicates that the buckling load for cylinders loaded in compression would change by only 1 percent if the boundary conditions of appendix B were used in lieu of the simple-support assumption.

Selected strain-gage data from gages mounted on the test cylinders are given in figure 7. The curves denoting strains in the corrugated walls of the cylinders were obtained in each instance by averaging strains from gages located on the inside and outside surfaces of the cylinders. Strains from corresponding inside and outside gages were in every instance nearly equal; this indicates that the flat plate elements which make up the corrugated wall were not subjected to local buckling.

Strain gages were located on troughs or crests of the corrugations rather than on the neutral axis of the wall. Hence, readings from the gages can be used as an indication of bending of the wall – that is, experimental strains which increase at a different rate from that of the calculated strains presumably indicate that the wall is subjected to bending at that location. For the gages shown in figure 7, strain rates greater than the calculated rate denote outward bending of the wall and rates less than the calculated value denote inward bending.

The plots of figure 7 indicate that some of the test cylinders experienced considerable wall bending during application of load. Evidently, initial imperfections (buckles) existed before the start of loading and caused bending of the wall during application of load. In most instances, the initial imperfections did not appear to grow appreciably in depth until the buckling load was approached. (Growth of imperfections is presumed to be synonymous with nonlinearity of the load-strain curve.) At loads approaching the buckling load, some of the imperfections began to grow in depth, whereas others reversed direction to form the buckled configuration.

It is not clear from the strain-gage data whether or not initial imperfections had much influence in determining the magnitude of the buckling load. The most nonlinearity at low loads occurred for cylinder 1. Agreement between theory and test for this cylinder is the best of all the cylinders tested (fig. 5). However, cylinder 1 buckled in the

panel-instability mode and it is generally known that the panel-instability load is not particularly susceptible to initial imperfections because of its close relationship to the Euler column load of a flat corrugated plate. On the other hand, agreement between theory and test for cylinder 1 in the general-instability mode is as good as the agreement obtained for the other cylinders in spite of the existence of panel-instability-type buckles of sufficient depth to be noticeable under careful visual observation. It appears therefore that the imperfections, or more precisely the prebuckling deformations in this instance, did not have a very detrimental effect on the buckling load. More general conclusions regarding the effect of prebuckling deformations cannot be made on the basis of the tests conducted. Prebuckling deformations arising from ring restraint resemble those arising from panel instability in that both deformations consist of a bulging of the corrugated wall between rings. Their effect on the general-instability load of corrugated cylinders has not been investigated. The effect of such deformations has been investigated only for conventional thin-wall cylinders where it was found to be important (refs. 13 to 15).

Some evidence regarding the number of longitudinal half-waves into which the cylinders buckled can be gleaned from the data of figure 7. The data indicate that the cylinders usually buckled into more waves than predicted by theory. A notable exception is cylinder 1; the data indicate buckling into the panel-instability mode as predicted for this cylinder. The other cylinders appear to have buckled into one half-wave more than predicted although definite conclusions cannot be drawn on this point because insufficient stations were monitored to reproduce the shape of the complete buckle pattern.

Some strain-gage data on reinforcing rings are also given in figure 7. These data indicate that the rings are normally subjected to only rather small bending strains, and to even smaller membrane strains, before the onset of buckling of the cylinder.

CONCLUDING REMARKS

The results of buckling tests on five corrugated ring-stiffened cylinders and the corresponding analysis indicate that buckling in the general-instability mode occurred at a load approximately 75 percent of the predicted buckling load; the prediction was based on a small-deflection buckling analysis (NASA TN D-3351) which considers the one-sidedness of reinforcing members as well as the difference between the buckling load of cylinders loaded in bending and that of cylinders loaded in uniform axial compression. The reason for the lower general-instability loads was not determined from the investigation but is probably associated with prebuckling deformations and with differences in boundary conditions employed in the theory and those existing in the test cylinders. These

phenomena, which are known to influence the buckling load of conventional thin-wall cylinders, have not been investigated for corrugated ring-stiffened cylinders. Buckling in the panel-instability mode was adequately predicted by the analysis.

Langley Research Center,
National Aeronautics and Space Administration,
Langley Station, Hampton, Va., January 14, 1966.

APPENDIX A

CONVERSION OF U.S. CUSTOMARY UNITS TO SI UNITS

The International System of Units (SI) was adopted by the Eleventh General Conference on Weights and Measures, Paris, October 1960, in Resolution No. 12 (ref. 5). Conversion factors for the units used in this report are given in the following table:

Physical quantity	U.S. Customary Unit	Conversion factor (*)	SI Unit
Length	in.	0.0254	meters (m)
Stress, modulus . . .	ksi	6.895×10^6	newtons/meter^2 (N/m^2)
Moment	in-kips	113.0	meter-newtons (m-N)

*Multiply value given in U.S. Customary Unit by conversion factor to obtain value in SI Unit.

Prefixes to indicate multiple of units are as follows:

Prefix	Multiple
giga (G)	10^9
kilo (k)	10^3
centi (c)	10^{-2}
milli (m)	10^{-3}

APPENDIX B

INFLUENCE OF RING RESTRAINT ON THE PANEL-INSTABILITY LOAD OF CORRUGATED CYLINDERS IN AXIAL COMPRESSION

The stiffness properties of ring-stiffened corrugated cylinders are such that curvature has very little effect on the buckling strength of the cylinders if buckling takes place between rings. Hence, the panel-instability load can be predicted rather accurately with the use of the Euler column equation. Ring deformation in the panel-instability mode entails a rolling of the ring by the cylinder wall, with the rolling resisted by the bending stiffness of the ring about an axis perpendicular to a generator of the cylinder (see ref. 16).

The condition for buckling of a corrugated cylinder with many equally spaced rings into the panel-instability mode (column mode) can be written as (see ref. 17)

$$2\left(\frac{M}{\theta}\right)_{cyl} + \left(\frac{M}{\theta}\right)_{ring} = 0 \tag{B1}$$

where $\left(\frac{M}{\theta}\right)_{cyl}$ is the "stiffness" of the cylinder wall in the panel-instability mode and can be obtained from equation (28) of reference 7 (p. 14) as

$$\left(\frac{M}{\theta}\right)_{cyl} = \frac{2D_x}{l}\,\frac{u}{\tan u} \tag{B2}$$

with

$$u = \frac{\pi}{2}\sqrt{\frac{N_x}{N_o}}$$

The stiffness of the reinforcing ring is given by (ref. 16, eq. (126))

$$\left(\frac{M}{\theta}\right)_{ring} = \frac{EI_{ring}}{R^2} \tag{B3}$$

The panel-instability load is obtained by substituting equations (B2) and (B3) into equation (B1) and solving for the load N_x that satisfies equation (B1).

REFERENCES

1. Sterett, James B., Jr.: Shell Stability Problems in the Design of Large Space Vehicle Boosters. Collected Papers on Instability of Shell Structures – 1962, NASA TN D-1510, 1962, pp. 57-66.

2. Hedgepeth, John M.; and Hall, David B.: Stability of Stiffened Cylinders. AIAA J., vol. 3, no. 12, Dec. 1965, pp. 2275-2286.

3. Block, David L.; Card, Michael F.; and Mikulas, Martin M., Jr.: Buckling of Eccentrically Stiffened Orthotropic Cylinders. NASA TN D-2960, 1965.

4. Block, David L.: Buckling of Eccentrically Stiffened Orthotropic Cylinders Under Pure Bending. NASA TN D-3351, 1966.

5. Mechtly, E. A.: The International System of Units – Physical Constants and Conversion Factors. NASA SP-7012, 1964.

6. Hu, Pai C.; Lundquist, Eugene E.; and Batdorf, S. B.: Effect of Small Deviations From Flatness on Effective Width and Buckling of Plates in Compression. NACA TN 1124, 1946.

7. Timoshenko, S.: Theory of Elastic Stability. McGraw-Hill Book Co., Inc., 1936.

8. Bijlaard, P. P.; and Gallagher, R. H.: Elastic Instability of a Cylindrical Shell Under Arbitrary Circumferential Variation of Axial Stress. J. Aerospace Sci., vol. 27, no. 11, Nov. 1960, pp. 854-858, 866.

9. Seide, Paul; and Weingarten, V. I.: On the Buckling of Circular Cylindrical Shells Under Pure Bending. Trans. ASME, Ser. E: J. Appl. Mech., vol. 28, no. 1, Mar. 1961, pp. 112-116.

10. Gellatly, R. A.; and Gallagher, R. H.: Sandwich Cylinder Instability Under Nonuniform Axial Stress. AIAA J. (Tech. Notes), vol. 2, no. 2, Feb. 1964, pp. 398-400.

11. Stroud, W. Jefferson: Elastic Constants for Bending and Twisting of Corrugation-Stiffened Panels. NASA TR R-166, 1963.

12. Block, David L.: Influence of Ring Stiffeners on Instability of Orthotropic Cylinders in Axial Compression. NASA TN D-2482, 1964.

13. Stein, Manuel: The Influence of Prebuckling Deformations and Stresses on the Buckling of Perfect Cylinders. NASA TR R-190, 1964.

14. Fischer, G.: Über den Einfluss der gelenkigen Lagerung auf die Stabilität dünnwandiger Kreiszylinderschalen unter Axiallast und Innendruck. Z. Flugwissenschaften, Jahrg. 11, Heft 3, Mar. 1963, pp. 111-119.

15. Almroth, B. O.: Influence of Edge Conditions on the Stability of Axially Compressed Cylindrical Shells. NASA CR-161, 1965.

16. Timoshenko, S.: Strength of Materials. Part II – Advanced Theory and Problems. Third ed., D. Van Nostrand Co., Inc., c.1956, pp. 138-139.

17. Lundquist, Eugene E.; Stowell, Elbridge Z.; and Schuette, Evan H.: Principles of Moment Distribution Applied to Stability of Structures Composed of Bars or Plates. NACA Rept. 809, 1945. (Supersedes NACA WR L-326.)

TABLE I.- DIMENSIONS AND TEST RESULTS OF CYLINDERS

(a) U.S. Customary Units

Cylinder	t, in.	l, in.	M_{cr}, in-kips		M_{ult}, in-kips
			Panel	General	
1	0.0211	20.0	1650	2050	2190
2	.0211	13.3	----	2300	2440
3	.0210	10.0	----	2850	2910
4	.0210	8.0	----	3100	3320
5	.0208	4.0	----	4200	4310

(b) SI Units

Cylinder	t, mm	l, cm	M_{cr}, km-N		M_{ult}, km-N
			Panel	General	
1	0.536	50.8	186	232	247
2	.536	33.8	---	260	276
3	.533	25.4	---	322	329
4	.533	20.3	---	350	375
5	.528	10.2	---	475	487

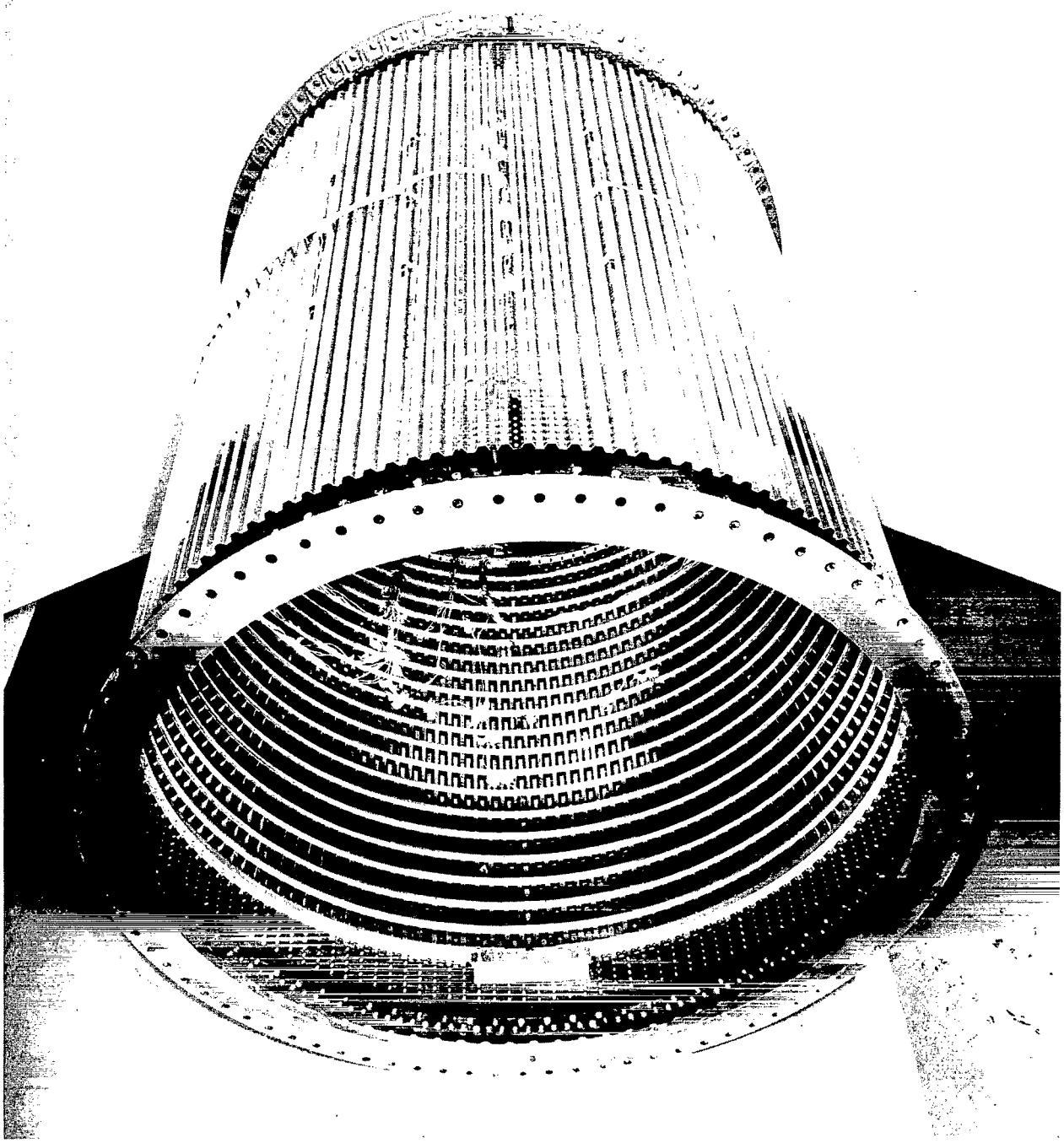

(a) General view.

L-65-3340

Figure 1.- Corrugated test cylinder.

(b) View of reinforcing rings. L-65-3342

Figure 1.- Concluded.

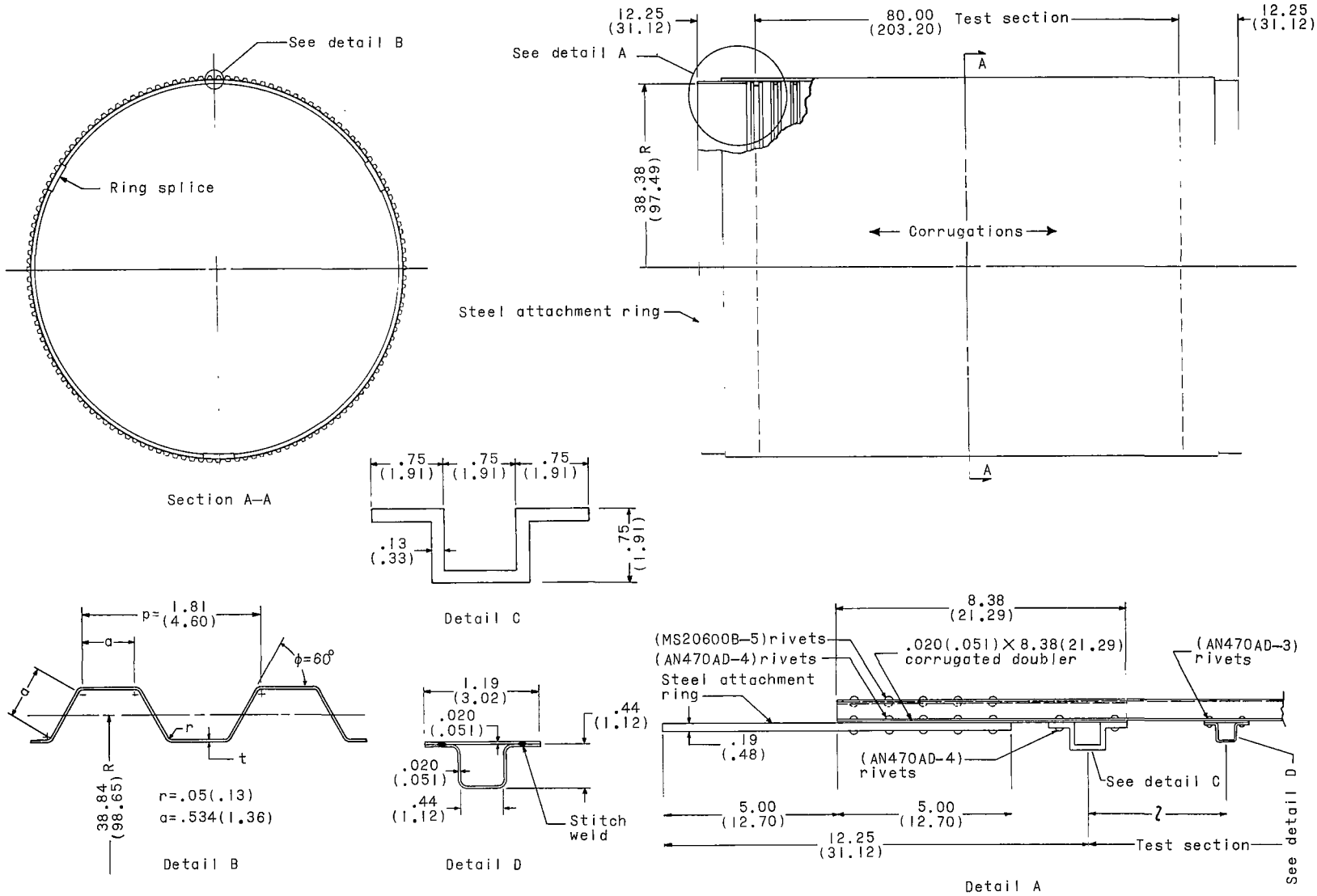

Figure 2.- Details of test cylinders. Dimensions are in inches (centimeters).

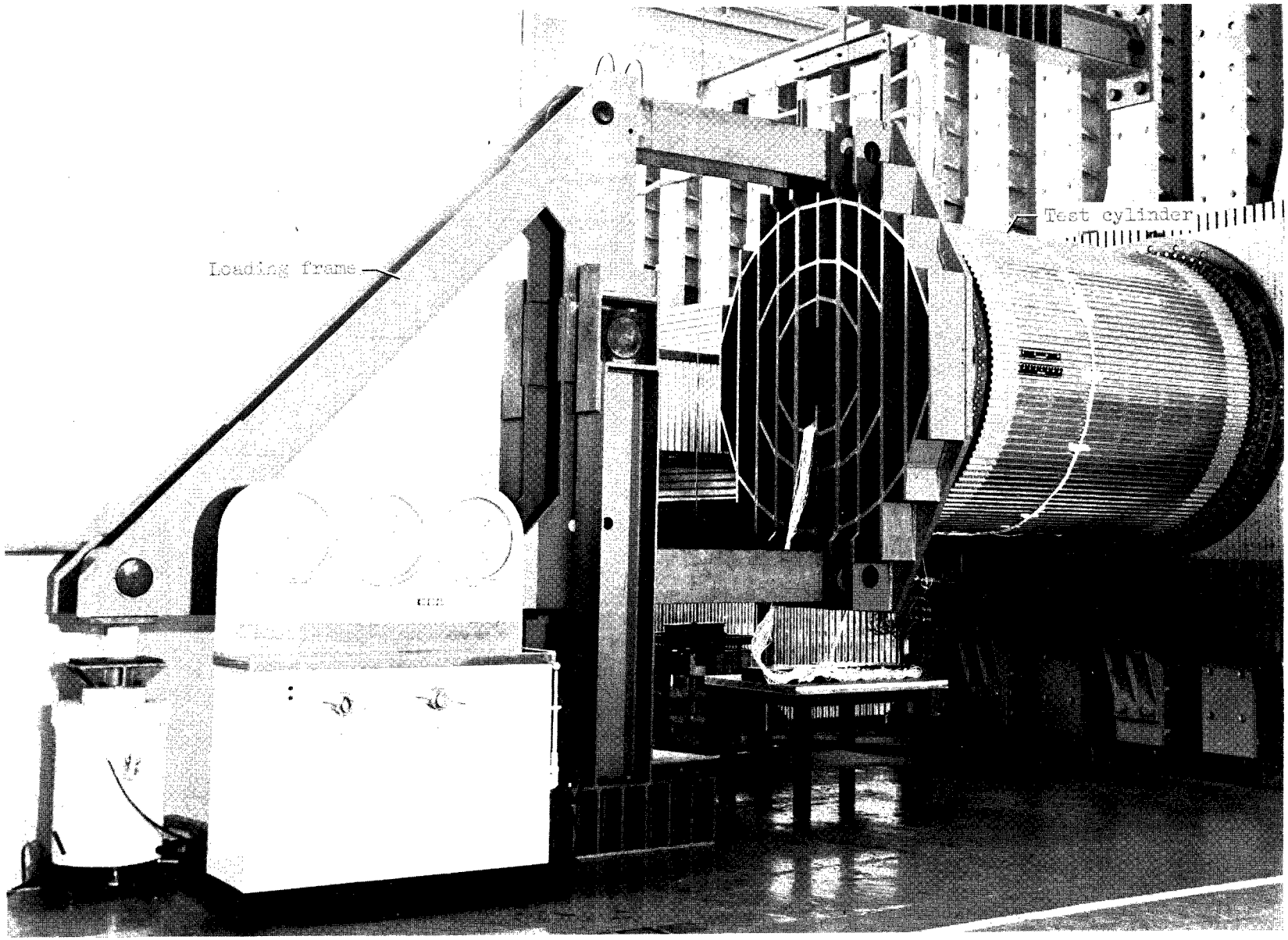

Figure 3.- Setup for bending tests on ring-stiffened corrugated cylinders. L-64-8855.1

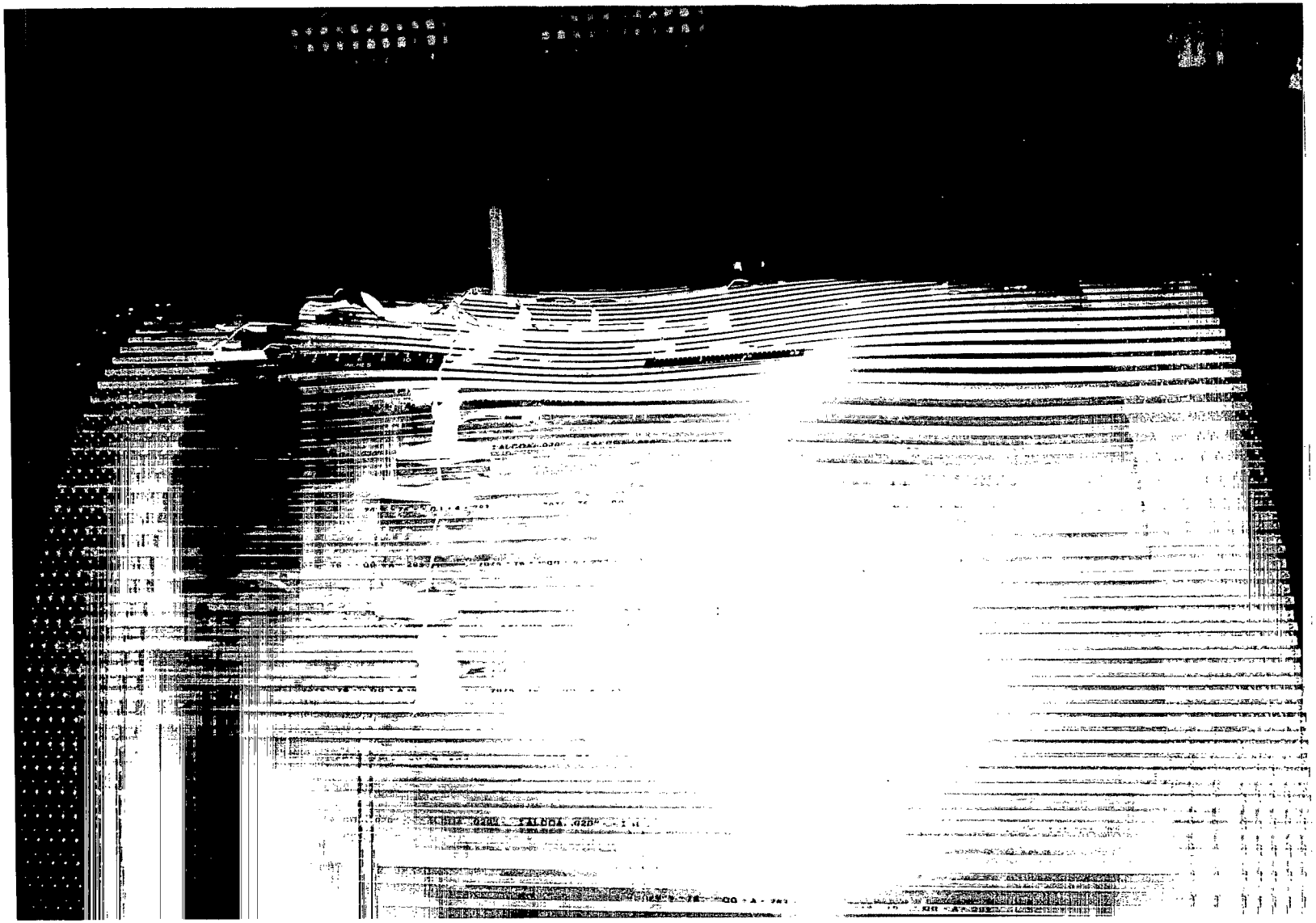

(a) Cylinder 1.

L-64-10,868

Figure 4.- Failure of test cylinders.

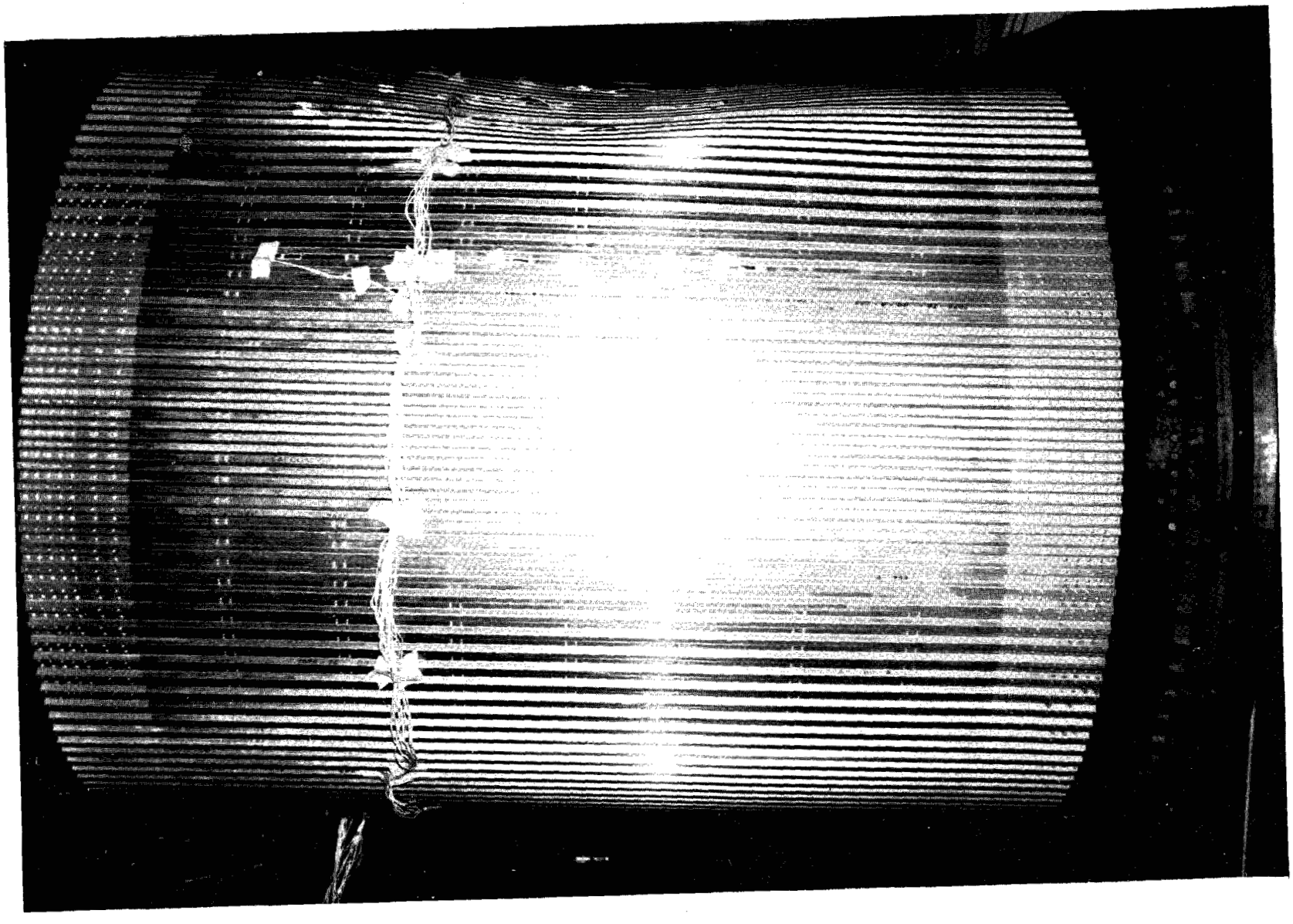

(b) Cylinder 3.

L-64-11,513

Figure 4.- Continued.

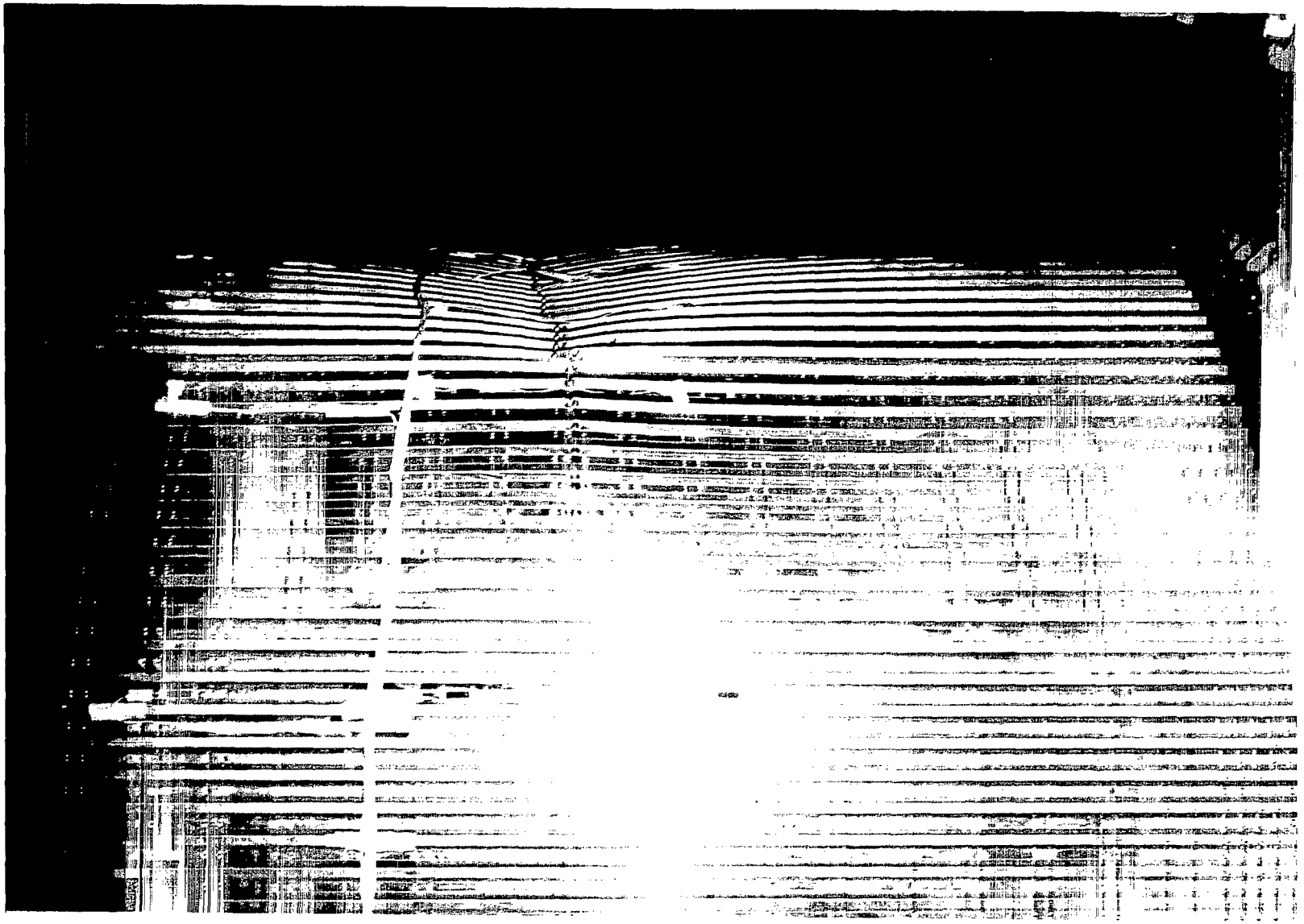

(c) Cylinder 5.

L-65-4801

Figure 4.- Concluded.

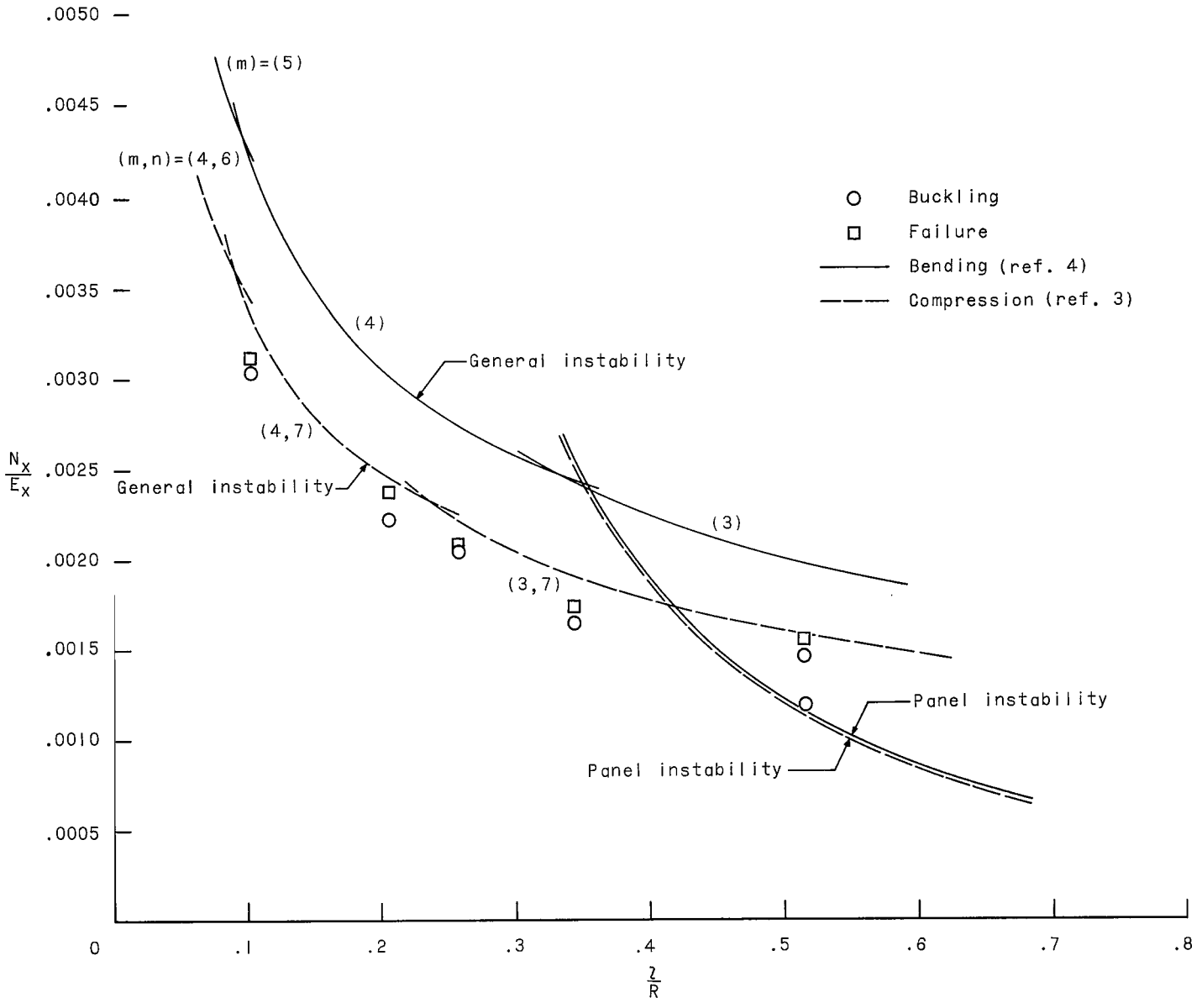

Figure 5.- Comparison between measured and calculated buckling loads for test cylinders.

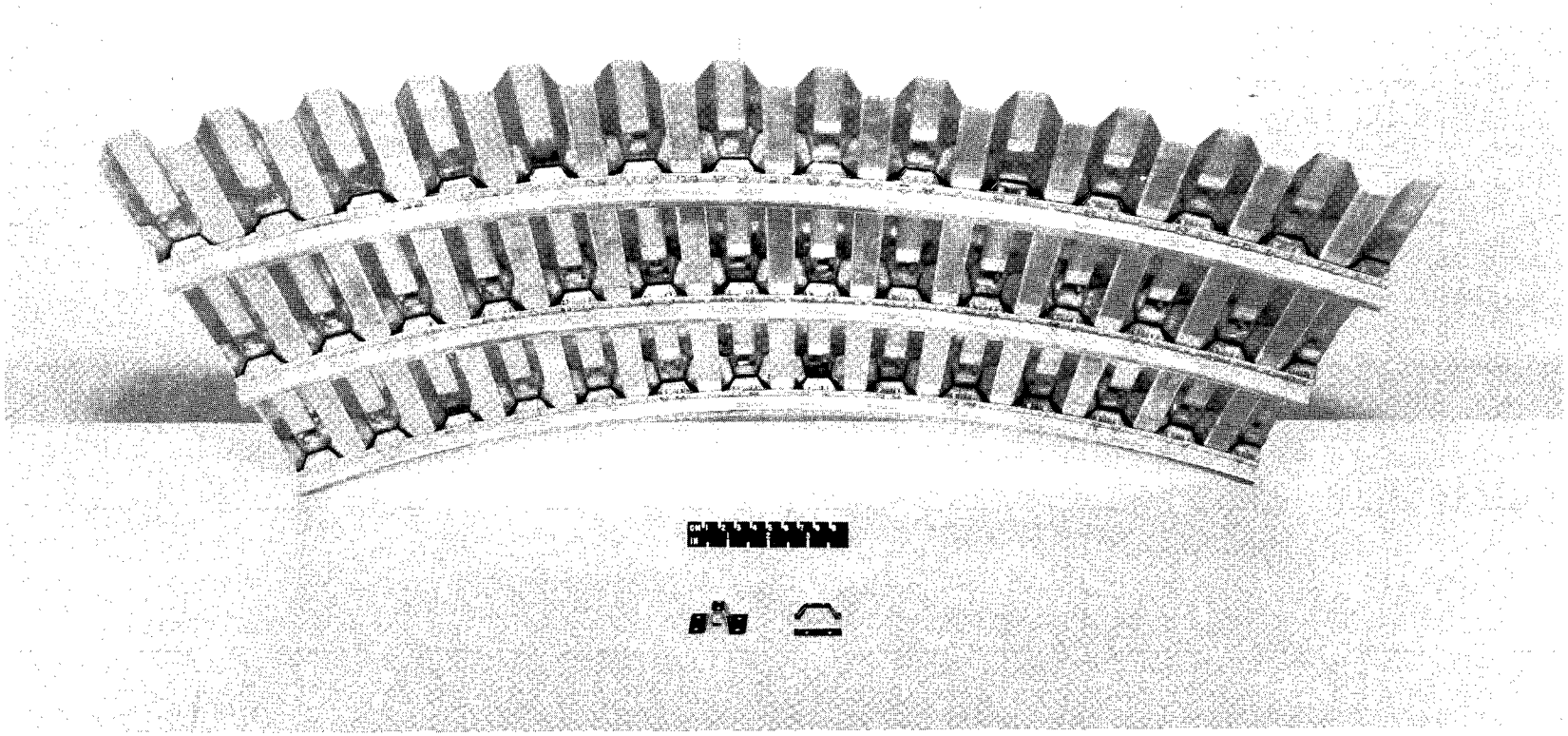

Figure 6.- Attachment between corrugated wall and reinforcing rings for auxiliary test. L-65-6899

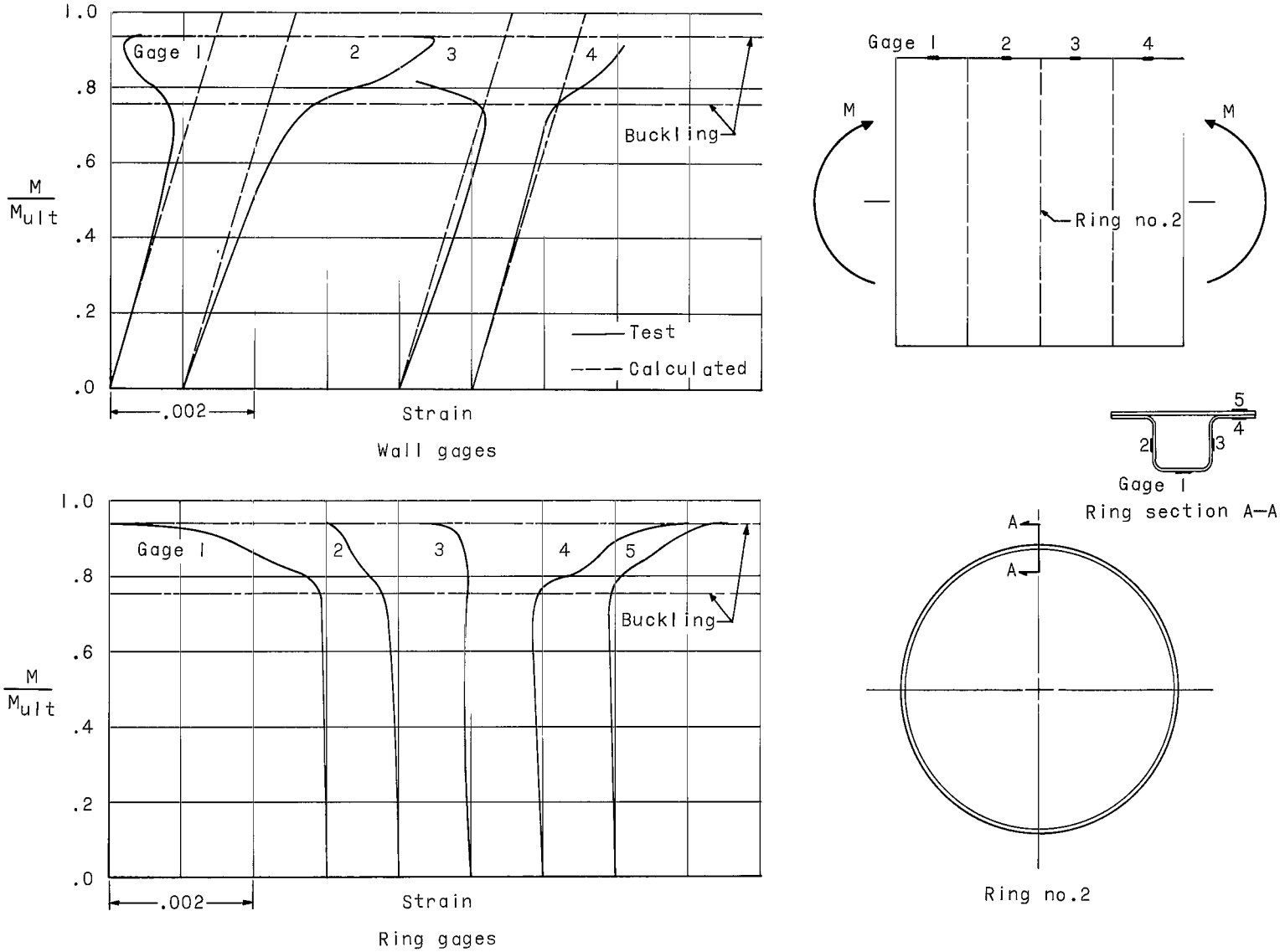

(a) Cylinder 1.

Figure 7.- Measured strains in test cylinders.

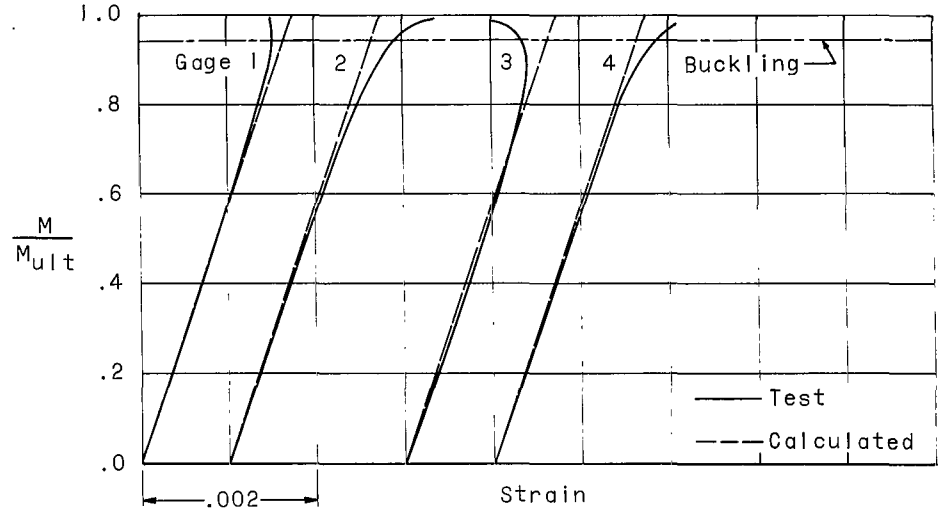

Wall gages

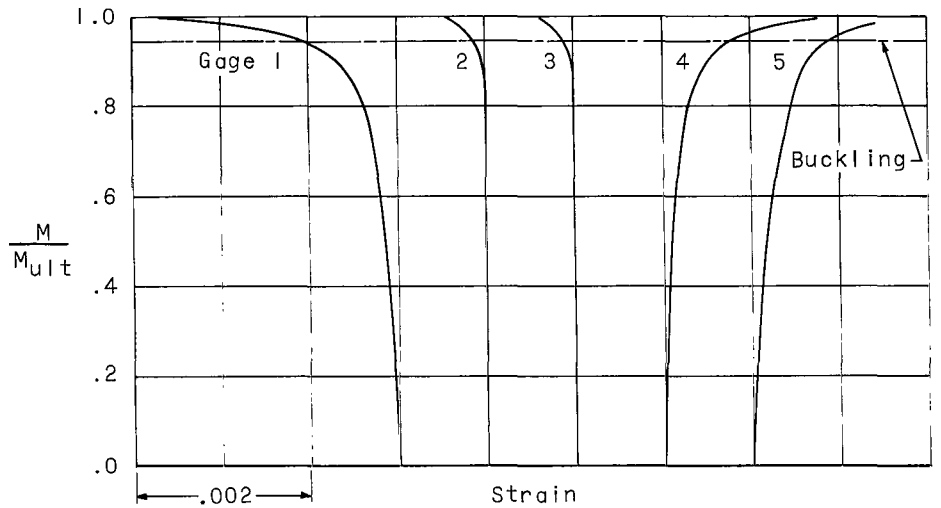

Ring gages

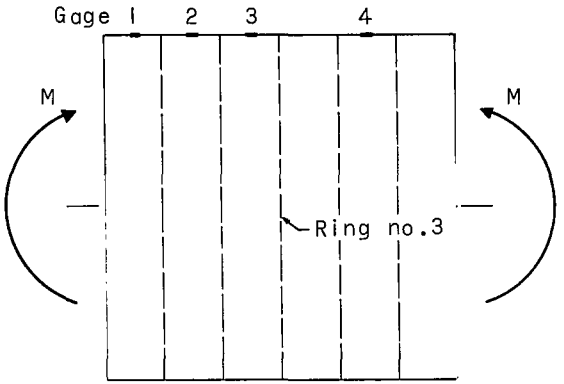

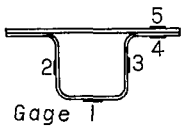

Ring section A–A

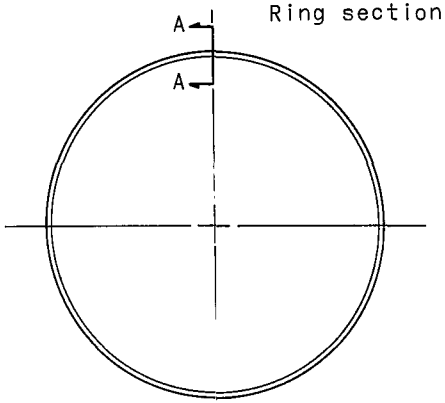

Ring no. 3

(b) Cylinder 2.

Figure 7.- Continued.

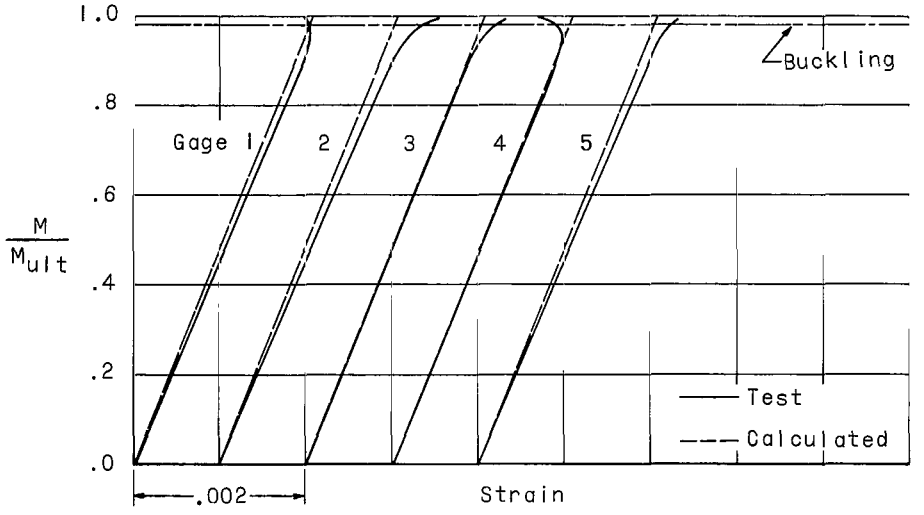

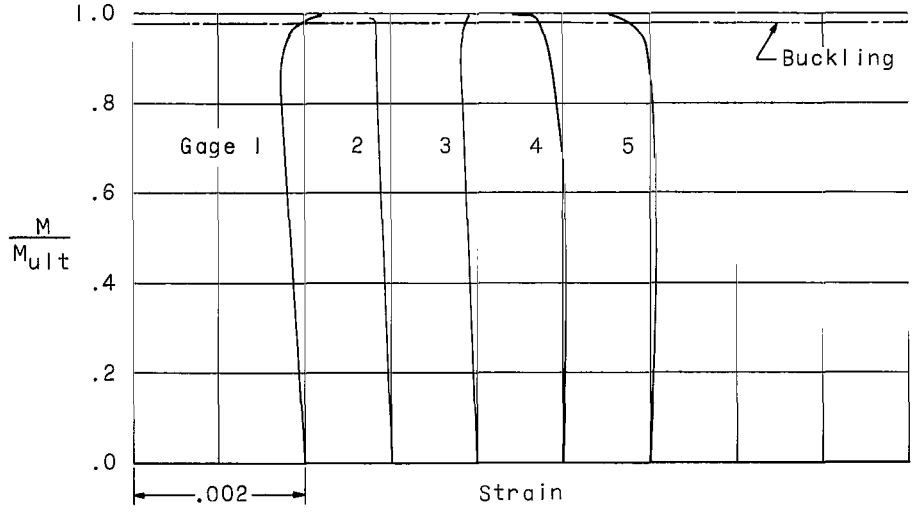

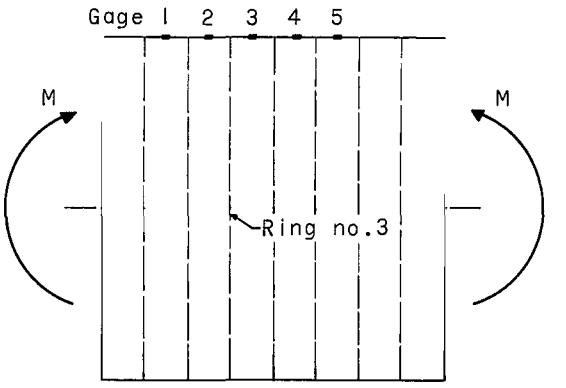

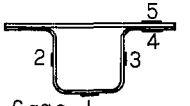

Ring section A–A

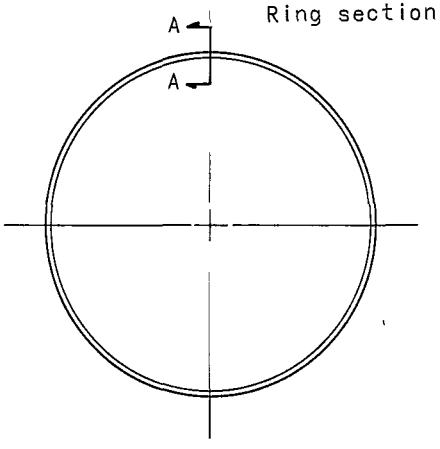

(c) Cylinder 3.

Figure 7.- Continued.

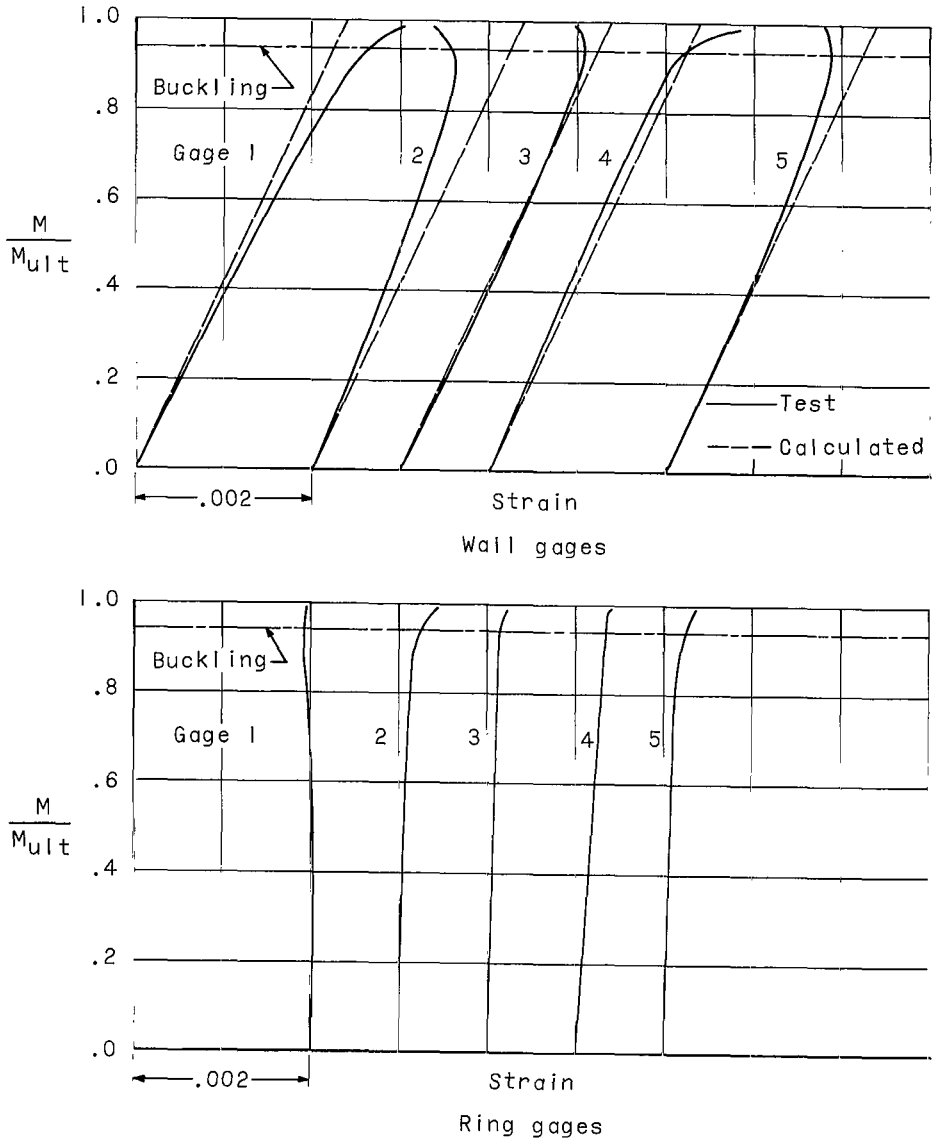

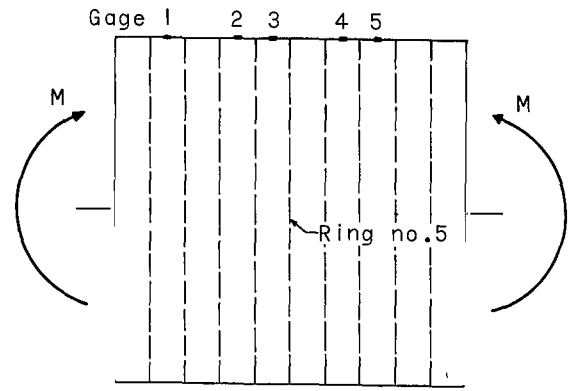

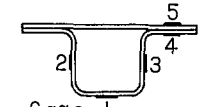

Ring section A–A

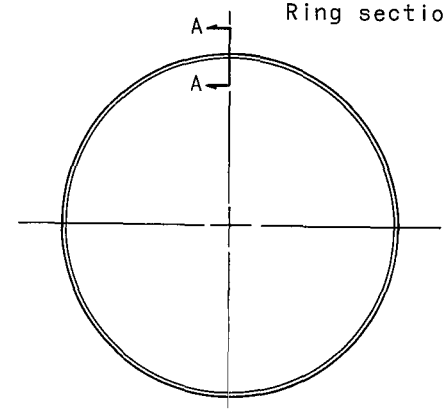

Ring no.5

(d) Cylinder 4.

Figure 7.- Continued.

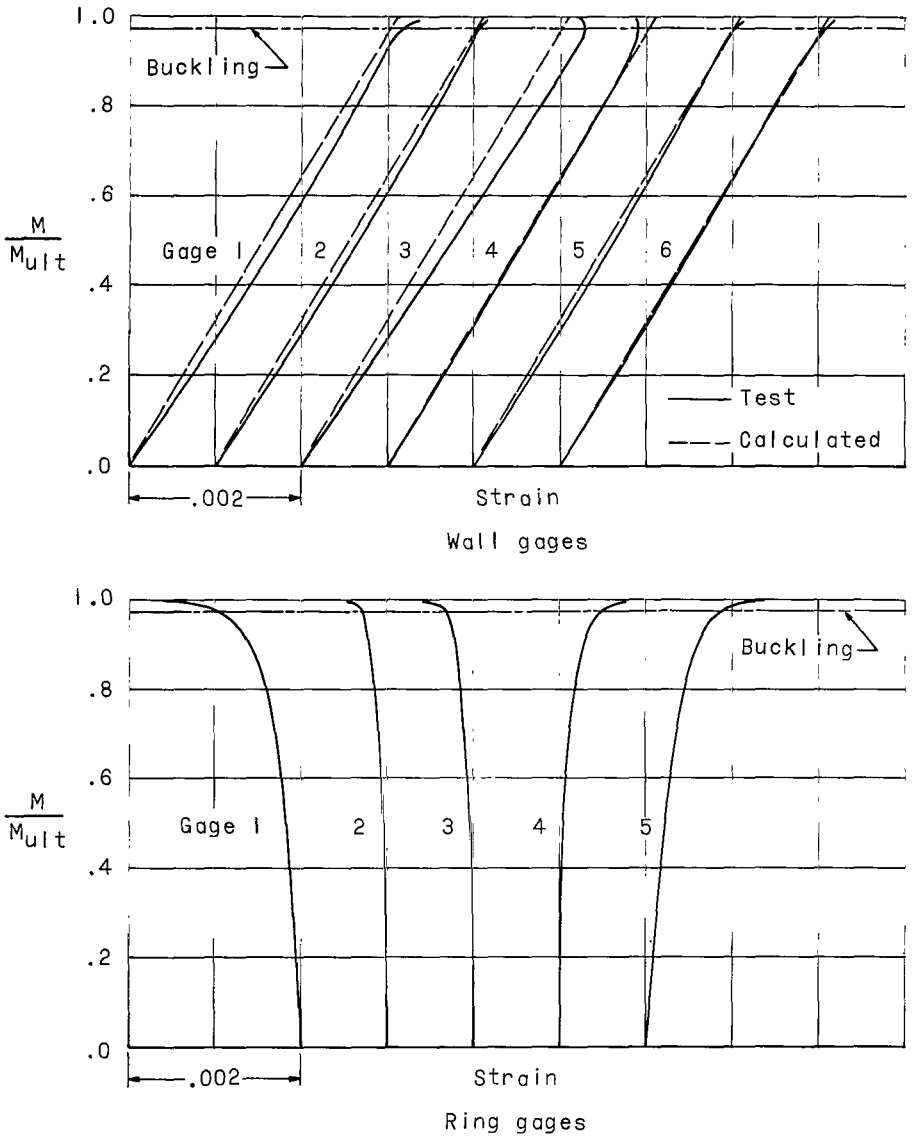

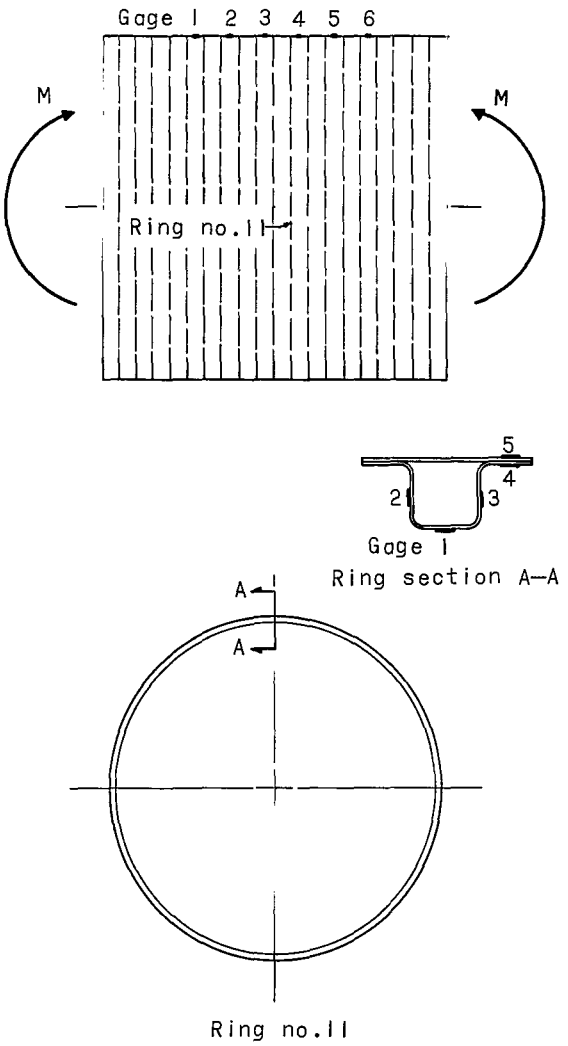

(e) Cylinder 5.

Figure 7.- Concluded.

"The aeronautical and space activities of the United States shall be conducted so as to contribute . . . to the expansion of human knowledge of phenomena in the atmosphere and space. The Administration shall provide for the widest practicable and appropriate dissemination of information concerning its activities and the results thereof."

—NATIONAL AERONAUTICS AND SPACE ACT OF 1958

NASA SCIENTIFIC AND TECHNICAL PUBLICATIONS

TECHNICAL REPORTS: Scientific and technical information considered important, complete, and a lasting contribution to existing knowledge.

TECHNICAL NOTES: Information less broad in scope but nevertheless of importance as a contribution to existing knowledge.

TECHNICAL MEMORANDUMS: Information receiving limited distribution because of preliminary data, security classification, or other reasons.

CONTRACTOR REPORTS: Technical information generated in connection with a NASA contract or grant and released under NASA auspices.

TECHNICAL TRANSLATIONS: Information published in a foreign language considered to merit NASA distribution in English.

TECHNICAL REPRINTS: Information derived from NASA activities and initially published in the form of journal articles.

SPECIAL PUBLICATIONS: Information derived from or of value to NASA activities but not necessarily reporting the results of individual NASA-programmed scientific efforts. Publications include conference proceedings, monographs, data compilations, handbooks, sourcebooks, and special bibliographies.

Details on the availability of these publications may be obtained from:

SCIENTIFIC AND TECHNICAL INFORMATION DIVISION

NATIONAL AERONAUTICS AND SPACE ADMINISTRATION

Washington, D.C. 20546